Fabrication and Characterization of Advanced Triple-junction Amorphous Silicon Based Solar Cells

PHASE II – Quarter 1

Quarterly Technical Progress Report

March 1, 2006 to May 31, 2006

NREL Subcontract No. ZXL-5-44205-06

Subcontractor: The University of Toledo

Principal Investigator: Xunming Deng
(419) 530-4782; dengx@physics.utoledo.edu

Co-Principal Investigator: Robert W. Collins
(419) 530-2195; rcollins@physics.utoledo.edu

Department of Physics and Astronomy
University of Toledo, Toledo, OH 43606

Contract technical monitor: Dr. Bolko von Roedern

Table of Contents

Section 1

Executive Summary

This quarterly technical progress report covers the highlights of the research activities and results on the project of "The Fabrication and Characterization of High-efficiency Triple-junction a-Si Based Solar Cells" at the University of Toledo for the Period of March 1, 2006 to May 31, 2006, under NREL TFPPP subcontract number ZXL-5-44205-06.

Following this Executive Summary are three sections describing research performed during this quarter related to the tasks under this subcontract. The major technical progresses of these sections are summarized as follows:

Section 2: Effect of ZnO deposition condition for back reflector on the performance of nano-crystalline silicon solar cell

This work focused on the optimization of ZnO as a part of back reflector (BR) for nano-crystalline (nc-Si:H) and amorphous silicon (a-SiGe:H) thin film solar cells. The effect of deposition temperature of ZnO on film morphology and as a part of BR on the performance of nc-Si:H solar cell has been analyzed. We have found that the nano-crystalline silicon solar cells on BRs with ZnO films deposited at 120ºC have low FF and low J_{sc} but high V_{oc}. The reason of this phenomenon may be that the low temperature deposited ZnO film causes the nano-crystalline silicon film to have more amorphous phase. But when the ZnO is deposited at high temperature (350ºC), lots of crystallite rods show up, this can cause shunting problem to the solar cells. Based on the BR with ZnO deposited at 280ºC, we have fabricated a-Si:H / a-SiGe:H / nc-Si:H n-i-p triple junction solar cells with efficiency of 12.5%.

Section 3: Origin of optical losses in Ag/ZnO back-reflectors for thin film Si photovoltaics

For an improved understanding of optical losses in Ag/ZnO back-reflectors for thin film Si photovoltaics we have analyzed the structural evolution of the Ag film as well as interface formation with ZnO by real time spectroscopic ellipsometry (RTSE). We start by depositing a Ag film that exhibits the minimum surface roughness in order to determine interface optical losses under a best-case scenario. Then controlled microscopic roughness on the Ag is introduced to assess differences in the optical losses while remaining within the specular regime. The role of macroscopic roughness is treated in a separate section of this report.

Section 4: Optical Analysis of Textured Back-Reflectors and Overlying Si:H Deposition

In the accompanying report on the optics of back-reflectors used in Si-based thin film solar cells, ultrasmooth layers of Ag were prepared, ZnO was overdeposited, and the losses that occur in this ideal situation were characterized. In the present study, the optical structure of the real Ag/ZnO interface, including microscopic roughness and macroscopic roughness (i.e., texture, roughness on the scale of the wavelength) is analyzed using a laminar film model. The intent of this work is to understand and quantify the losses in the full range of Ag/ZnO structures from the ideal to the fully textured. Future work will involve characterization of single and multijunction a-Si:H-based solar cells on textured back-reflector substrates, including the capability of extracting the i-layer band gaps and crystallite volume fraction for layers intentionally deposited as microcrystalline Si:H.

Section 2

Effect of ZnO deposition condition for back reflector on the performance of nano-crystalline silicon solar cell

Xiesen Yang, Xinmin Cao, Wenhui Du, Chandan Das, Yasuaki Ishikawa, Lauri Edwards, Xunming Deng
Department of Physics and Astronomy, University of Toledo, Toledo, OH 43606, USA

1. INTRODUCTION

The purpose of the back reflector for thin film solar cell is to trap the photons of long wavelength and thus improve the current generated by the bottom cell [1,2]. The BR normally consists of highly reflective metal layer (Al or / and Ag) and ZnO buffer layer. It is important to optimize the texture of the BR to improve the light trapping [3, 4]. At the same time morphology of ZnO is also important since it acts as a direct substrate for the growth of Si thin film. It is known that the nc-Si:H microstructure is critically substrate-dependent [5]. The film morphology of ZnO is mainly determined by the deposition conditions of the sputter proc-ess [6]. Deposited at certain regime, although the ZnO films exhibit nearly similar transparency and resistivity, they show distinctly different surface morphologies [4, 7].

This work focuses on the optimization of ZnO as a part of back reflector (BR) for nano-crystalline (nc-Si:H) and amorphous silicon (a-SiGe:H) thin film solar cells. The effect of deposition temperature of ZnO on film morphology and as a part of BR on the performance of nc-Si:H solar cell has been analyzed.

2. EXPERIMENTAL

We fabricated BR's on stainless steel (SS) substrate by RF sputtering method. The complete structure of BR was SS / Al / Ag / ZnO. The Al and Ag metal layers, deposited at fixed conditions, provided high texture and reflectance. The ZnO films were deposited at four different substrate temperatures (120ºC, 200ºC, 280ºC, and 350ºC), keeping other conditions such as RF power (100W), Ar gas flow (4sccm), deposition pressure (p = 4 mTorr) and deposition time (t = 50 minutes) unchanged. The morphologies of the BR's surfaces were characterized by Scanning Electron Microscopy (SEM).

Standard nc-Si:H n-i-p single junction solar cells were deposited on BRs with ZnO deposited at different temperatures to see the effect of BR on cell performance. For comparison purpose we also fabricated n-i-p solar cell on control sample of BR (SS / Ag / ZnO) supplied by ECD in parallel with our BR sample. In addition to this we also fabricated triple junction a-Si:H / a-SiGe:H / nc-Si:H n-i-p solar cell on BR with ZnO deposited at 280ºC. Cells were characterized by quantum efficiency (QE) and J-V measurements.

3. RESULTS AND DISCUSSION

3.1 Surface Characterization of BR

Figure 1 shows the SEM image of the BR with ZnO deposited at 280ºC temperature. All the BRs exhibit similar texture with nearly micron size features independent of the deposition temperature of ZnO. This can be explained by the Al layer deposited underneath, which is responsible for the texture of these films. On the other hand morphology of ZnO films deposited at different temperatures is different. SEM data also show that the films deposited at lower temperature have smaller grain size than the films deposited at higher temperature. We hope to confirm this by X-ray diffraction.

The SEM image of the BR with ZnO deposited at 350ºC shows a large number of crystallite ZnO rods. These rods can cause low yield of the nc-Si:H solar cells; so we do not have solar cells deposited on BR with ZnO deposited at 350ºC.

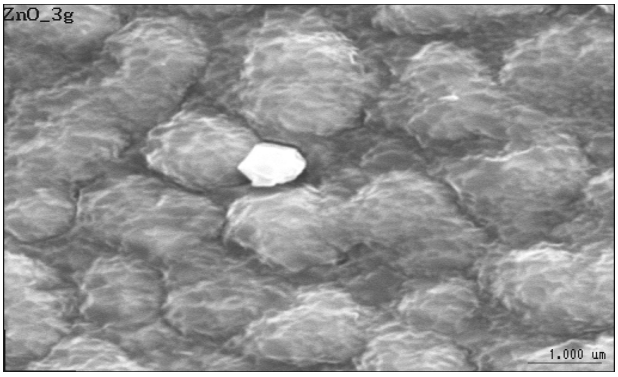

Figure 1: SEM image of surface of BR with ZnO layer deposited at: 280ºC

3.2 Effect of BR on nc-Si:H Solar Cell

To compare the cell performance and evaluate the quality of our BR, we deposited standard nc-Si:H solar cell on control sample supplied by ECD, simultaneously with BR's fabricated here at the University of Toledo. Table 1 shows the J-V data of the above-mentioned samples.

Table 1: J-V data for nc-Si:H n-i-p single-junction cells on BRs with ZnO deposited at different temperatures and on control samples.

Cell Number	T_{sub} (ºC)	V_{oc} (V)	J_{sc} (mA/cm^2)	FF (%)	η (%)
ZnO-1	120	0.541	17.1	52.6	4.86
Control	-	0.518	21.4	60.0	6.68
ZnO-2	200	0.510	22.8	61.9	7.20
Control	-	0.512	21.6	64.1	7.08
ZnO-3	280	0.526	20.6	64.3	6.96
Control	-	0.516	19.7	65.4	6.65

From the J-V data in table 1, we can see that the cell with ZnO deposited at 120ºC, has low J_{sc} and low FF, but high V_{oc}. The low temperature deposited ZnO film on which the nano-crystalline silicon is deposited can explain this. As a result, nano-crystalline silicon has more amorphous phase, which gives high V_{oc}, but low J_{sc} and low FF in cell performance. From table 1, we can see that the cells with ZnO deposited at 200ºC and 280ºC both have better performance than their control samples.

The QE data of sample ZnO-1 also show a low spectral response in short and long wavelength range. While sample ZnO-2 and ZnO-3 both have better spectral response than their control samples. The QE curve in figure 2 shows that cell with ZnO deposited at 200ºC has a better spectral response in the long wavelength range than the control sample with a Ag/ZnO BR. This means the BR made under this condition is suitable for nc-Si:H cells with thick i-layers.

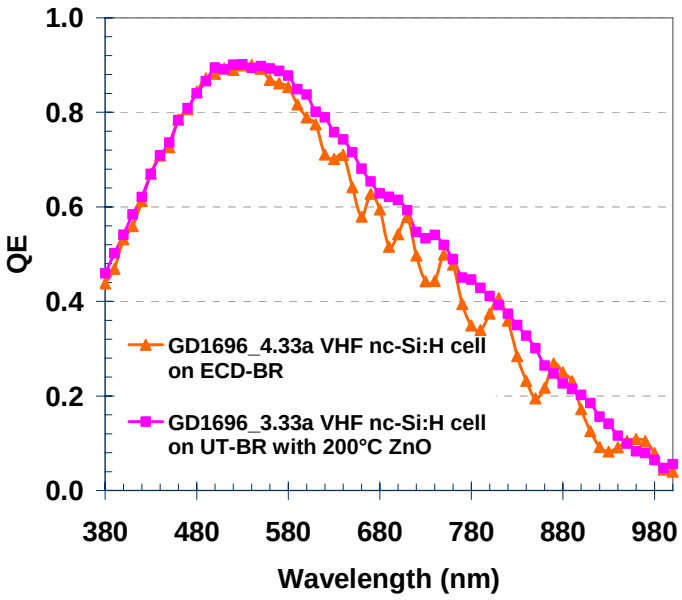

Figure 2: Quantum efficiency (QE) of nc-Si:H n-i-p solar cells deposited on BR with ZnO films deposited at 280ºC and on control sample.

Observing the similar performance of nc-Si:H n-i-p single-junction cell on BR's with ZnO deposited at 200ºC and 280ºC, we decided to fabricate a triple junction a-Si:H / a-SiGe:H / nc-Si:H n-i-p solar cell on a BR with ZnO deposited at 280ºC. Figure 3 shows the J-V curve of this triple junction cell. High power conversion efficiency of 12.5%, is achieved for this case.

Figure 4 shows the quantum efficiency data for this triple cell. The QE curve shows that this cell has a good spectral response at the overall wavelength range.

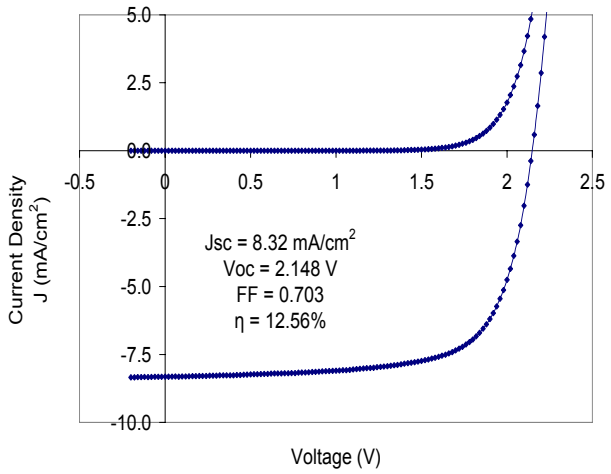

Figure 3: AM1.5 and dark J-V curves of triple junction n-i-p solar cell deposited on BR with ZnO film deposited at 280ºC.

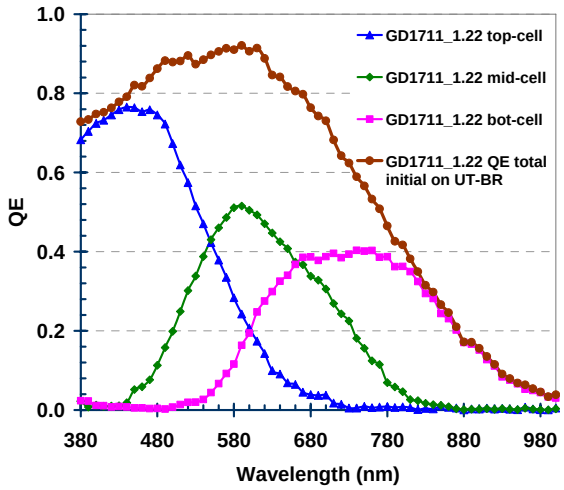

Figure 4: Quantum efficiency (QE) of triple junction n-i-p solar cell fabricated on BR with ZnO film deposited at 280ºC.

4. CONCLUSION

In this study, we have found that the nano-crystalline silicon solar cells on BRs with ZnO films deposited at 120ºC have low FF and low J_{sc} but high V_{oc}. The reason of this phenomenon may be that the low temperature deposited ZnO film causes the nano-crystalline silicon film to have more amorphous phase. But when the ZnO is deposited at high temperature (350ºC), lots of crystallite rods show up, this can cause shunting problem to the solar cells. Based on the BR with ZnO deposited at 280ºC, we have fabricated a-Si:H / a-SiGe:H / nc-Si:H n-i-p triple junction solar cells with efficiency of 12.5%.

5. ACKNOWLEDGEMENTS

This work was supported by the National Renewable Energy Laboratory “Thin Film Photovoltaic Partnership Program” under subcontract No. ZXL-5-44205-06.

6. REFERENCES

[1] H. W. Deckman, C.R. Wronski, H. Witzke and E. Yablonovitch, Appl. Phys. Lett. 42, 968 (1983).
[2] X. Deng, K. L. Narasimhan, First WCPEC; Dec. 5-9, 1994; Hawaii.
[3] O. Kluth, O. Vetterl, R. Carius, F. Finger, S. Wieder, B. Rech, H. Wagner, Mat. Res. Soc. Symp. Rroc. 557 (1999) 731
[4] B. Rech, H. Wagner, Appl. Phys., A 69 (1999) 155
[5] J. Koh, Y. Lee, H. Fujwara, C.R. Wronski, R.W. Collins, Appl. Phys. Lett. 73, 1526 (1998)
[6] K. H. Kin, K. C. Park, D. Y. M, J. Appl. Phys. 81 (12) (1997) 7764
[7] O. Kluth, B. Rech, L. Houben, S. Wieder, G. Schope, C. Beneking, H. Wagner, A.
[8] Loffl, H. W. Schock, Thin Solid Films 351 (1999) 247

Section 3

Origin of optical losses in Ag/ZnO back-reflectors for thin film Si photovoltaics

D. Sainju, P.J. van den Oever*, N. J. Podraza , J. Chen, J.A. Stoke, X. Yang, M. Syed,
R. W. Collins, and X. Deng

Department of Physics and Astronomy, University of Toledo, Toledo, OH 43606, USA
Dept. of Applied Physics, Eindhoven University of Technology, 5600 MB Eindhoven,
The Netherlands

Introduction

An effective back-reflector (BR) for thin film Si solar cells in the substrate/BR/n-i-p configuration consists of opaque Ag followed by ~3000 Å thick ZnO, both sputtered onto a low-cost substrate such as stainless steel. Quantum efficiency enhancement arises due to reflection of long wavelengths back into the cell for possible absorption in additional passes. Furthermore, the Ag/ZnO interface is designed to be macroscopically rough so that the rays are scattered upon back-reflection for increased optical path length. It is generally recognized that when macroscopic roughness is incorporated, however, absorption losses at the Ag/ZnO interface are enhanced; thus, the potential of the BR concept cannot be fully realized. For an improved understanding of these losses, we have analyzed the structural evolution of the Ag film as well as interface formation with ZnO by real time spectroscopic ellipsometry (RTSE). We start by depositing a Ag film that exhibits the minimum surface roughness in order to determine interface optical losses under a best-case scenario. Then controlled microscopic roughness on the Ag is introduced to assess differences in the optical losses while remaining within the specular regime. The role of macroscopic roughness is treated in a separate section of this report.

Experimental Details

The Ag films were deposited by magnetron sputtering onto c-Si wafer substrates covered with native and thermal oxides (d_{ox}~15-120 Å). Ultrasmooth Ag is achievable under optimum conditions using the c-Si/SiO_2, which is itself ultrasmooth. The smoothest Ag films exhibit a roughness thickness of d_s=6 Å, as deduced by RTSE at the end of the deposition (typically ~1500 Å in bulk layer thickness). These films are obtained at room temperature using the lowest gas pressure possible (~4 mTorr) and an intermediate target power (50 W). By elevating the substrate temperature to ~90°C, a much larger roughness layer thickness (but still microscopic and thus specular) of d_s=52 Å is obtained at the end of Ag deposition. ZnO was deposited at room temperature on the Ag surfaces having $6 \leq d_s \leq 52$ Å using the same sputtering conditions as for the Ag.

The rotating-compensator multichannel ellipsometer used here can provide spectra (0.75 to 6.5 eV) in (ψ, Δ) with a minimum acquisition time of 32 ms as an average over a single pair of optical cycles. Here, the spectra were collected in a time of ~1 s, as averages over ~30 optical cycle pairs in order to improve precision. During the acquisition time for one set of (ψ,Δ) spectra, a bulk layer thickness of ~6 Å accumulates at the maximum deposition rate for the Ag and ZnO films used here. Analyses of all spectra apply numerical inversion and least-squares regression algorithms. The incidence angle was 64.88±0.09°.

Results and discussions

Figure 1 shows the surface roughness evolution for Ag films sputtered onto oxidized c-Si at two temperatures, T = 20 and 87°C. At elevated T, a longer diffusion length of Ag on the SiO_2 is apparent; this gives rise to a lower nucleation density and a larger thickness at which nuclei make contact prior to coalescence. At low nucleation density, coalescence is incomplete, leaving residual roughness that is enhanced with increasing bulk layer thickness. By controlling T over the narrow range from 20 to 87°C, Ag films ~1500 Å thick with controlled roughness thicknesses d_s from 6 to 52 Å can be obtained.

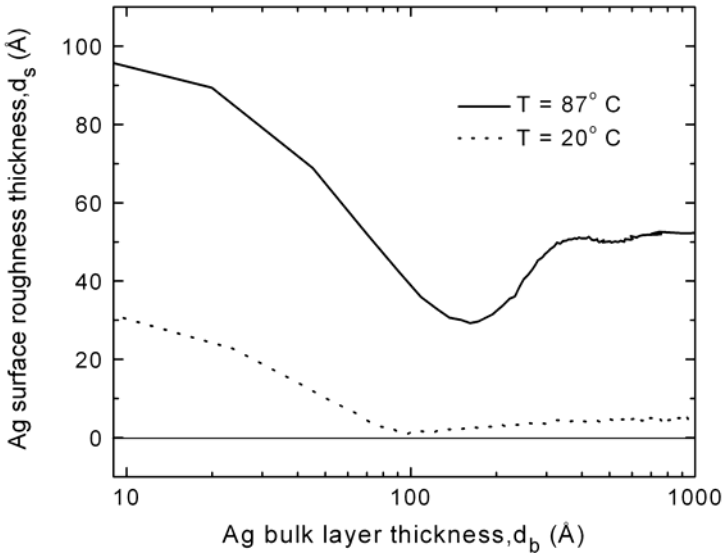

Fig. 1**:** Surface roughness evolution versus bulk layer thickness for Ag films sputtered onto oxidized Si at two temperatures, T = 20 and 87°C.

Figure 2 shows results for the evolution of ZnO bulk and interface layer thicknesses (d_b and d_i) in the first d_b ~ 300-400 Å of bulk layer growth on Ag surfaces having (a) d_s = 12 Å and (b) d_s = 27 Å. In the model for this process, the initial Ag roughness layer is subsumed by the interface layer, which is found to saturate at d_i ~ 50 - 70 Å after d_b ~200 Å. At the end of the ZnO

deposition, after d_b ~1500 Å, d_i has reached 60 - 80 Å; however, this final thickness shows no correlation with the roughness on the Ag. The range in d_i encompasses a value reported previously (70 Å) for a specular Ag/ZnO back-reflector fabricated in an industrial laboratory [1]. Evidently, the interface layer originates from a spontaneous reaction between Ag and ZnO that is unaffected by the Ag surface roughness, rather than from ion bombardment that would occur only in the early stages of interface formation.

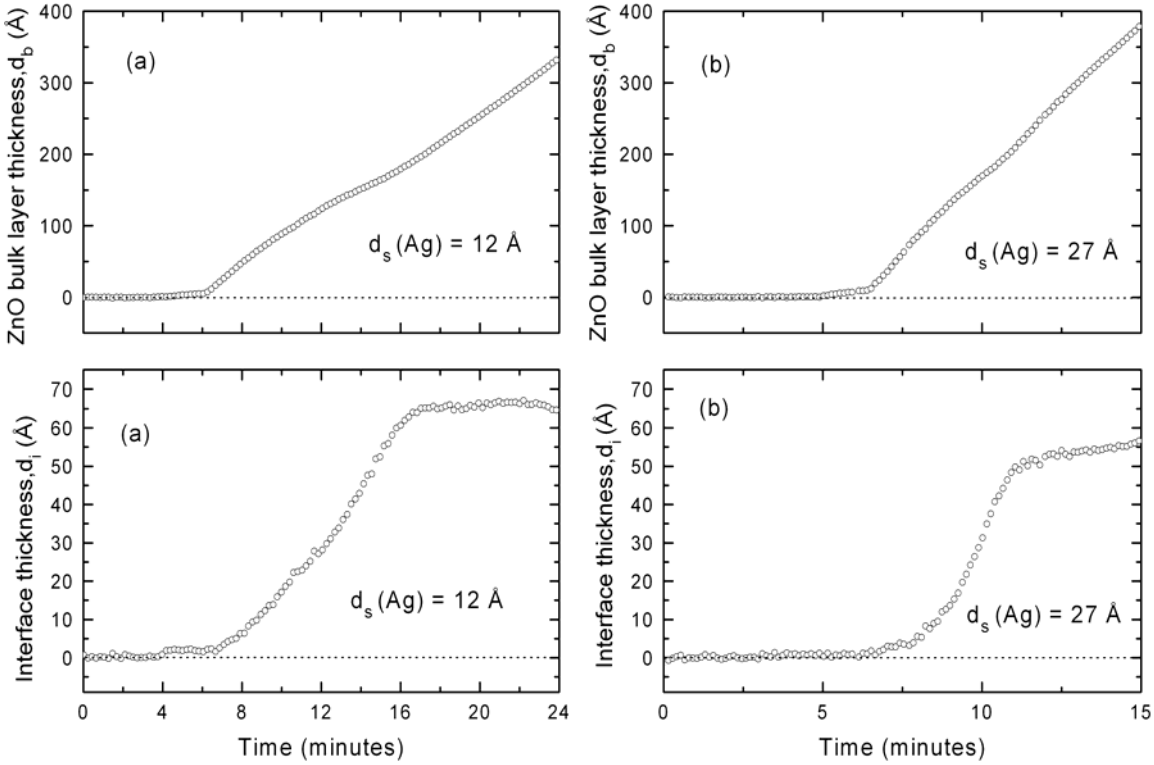

Fig. 2: Evolution of ZnO bulk and interface layer thicknesses in the first ~ 300 - 400 Å of bulk layer growth on Ag surfaces having (a) d_s = 12 Å and (b) d_s = 27 Å. The initial surface roughness on the Ag is subsumed into the interface layer.

Although the interface thickness is not correlated with the Ag roughness layer thickness, the interface optical properties exhibit a particle plasmon band whose amplitude tends to increase with d_s over the range of d_s explored here. Figure 3 shows the dielectric functions $\varepsilon = \varepsilon_1 + i\varepsilon_2$ of the interface layers for the sample structures of Fig. 2, deduced by inversion of ellipsometric spectra (points), along with fits using a Kramers-Kronig-consistent model (lines). The ability of the fits to reproduce the features in ε_1 and ε_2 supports the modeling approach. The interface layer model includes a free electron component (Drude), a particle plasmon band (Lorentz, peaked near 2.8 eV), and a bound electron absorption onset (Tauc-Lorentz, near 3.7 eV). The most obvious effect is an increase in the plasmon band amplitude with increasing d_s of the Ag. Figure 4(a) shows the measured reflectance for a Ag/ZnO structure in which d_s = 28 Å for the Ag. The reflectance is consistent with an optical model (dotted line) that includes an 80 Å interface layer, and reveals enhanced losses due to this interface layer for photon energies above

1.5 eV. The strong minimum in R at 2.6 eV is not observed in the ideal (d_i=0 Å) simulation (solid line). This minimum is caused by an interesting optical effect: interference-enhanced plasmon absorption. Figure 4(b) shows reflectance simulations for a thicker ZnO layer (d_b =

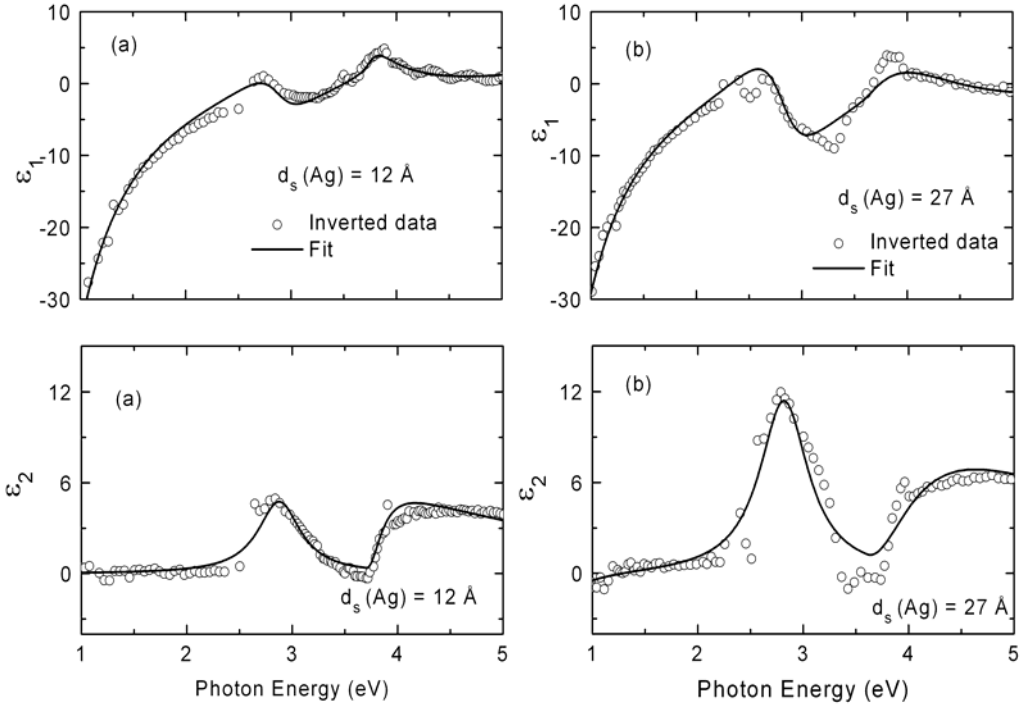

Fig. 3: The dielectric functions $\varepsilon = \varepsilon_1 + i\varepsilon_2$ of the interface layers for the sample structures of Fig. 2 in which the Ag surfaces exhibit (a) d_s = 12 Å and (b) d_s = 27 Å. Results from exact inversion of ellipsometric spectra (points) are shown along with a fit using a Kramers-Kronig- consistent optical model (lines).

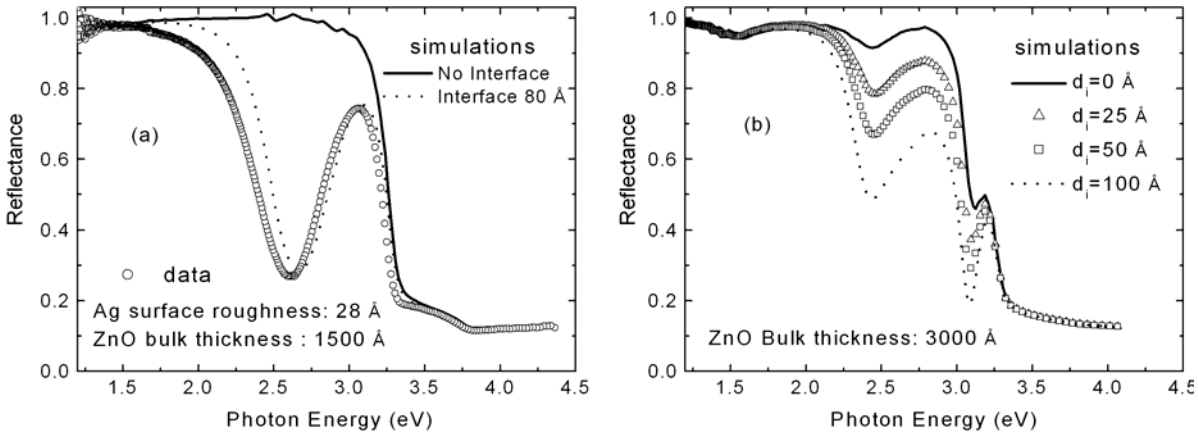

Fig. 4 (a) Reflectance data and simulations for a ZnO thickness of d_b = 1500 Å and interface layer thicknesses of d_i=0 and 80Å ; (b) reflectance simulations with d_b = 3000 Å and different d_i values.

3000 Å), demonstrating that the dominant losses in the interesting range of 1.2 to 1.5 eV are independent of d_i, and are due to intrinsic losses in the Ag, enhanced by interference.

The implications of these results for solar cell losses are discussed further in a separate section of this report and will be the subject of future report sections.

References

[1] G.M. Ferreira, A.S. Ferlauto, P.I. Rovira, C, Chen, H.V. Nguyen, C.R. Wronski, and R.W. Collins, *Mater. Res. Soc. Symp. Proc.* **664**, A24.6 (2001).

Section 4

Optical Analysis of Textured Back-Reflectors and Overlying Si:H Deposition

Jason A. Stoke, Deepak Sainju, Nikolas J. Podraza, Xunming Deng, and Robert Collins
Department of Physics and Astronomy, University of Toledo, Toledo, OH 43606

Introduction

In the accompanying report on the optics of back-reflectors used in Si-based thin film solar cells, ultrasmooth layers of Ag were prepared, ZnO was overdeposited, and the losses that occur in this ideal situation were characterized. Losses not associated with the bulk ZnO and Ag could be attributed to to a Ag/ZnO interface layer whose dielectric function reveals the characteristics of free electrons from the Ag component, bound electron resonances from the Ag and ZnO components, and plasmon resonances in Ag clusters that appear to form at the Ag/ZnO interface. Once the ideal interface is understood, then microscopic roughness (i.e., roughness with an in-plane scale less than the light wavelength) of increasing thickness can be introduced through variations in the Ag deposition temperature. In the present study, the optical structure of the real Ag/ZnO interface, including microscopic roughness and macroscopic roughness (i.e., texture, roughness on the scale of the wavelength) is analyzed using a laminar film model. The intent of this work is to understand and quantify the losses in the full range of Ag/ZnO structures from the ideal to the fully textured.

Experimental

The back-reflector used in this study was prepared at Energy Conversion Devices under standard conditions. An amorphous silicon (a-Si:H) n-layer was deposited on this backreflector and analyzed to determine whether thin layer growth can be characterized on standard textured transparent conducting oxide substrates. The uncoated back-reflector and the back-reflector with the thin n-layer were characterized by ex situ spectroscopic ellipsometry over the energy range from 0.75 to 6.5 eV, easily spanning the operating range of interest for the back-reflector.

Results and Discussion: Back-reflector and Losses

Figure 1 shows the ellipsometric spectra (points) for the back-reflector along with a best fit (lines) using the structure of Fig. 2. The reference dielectric functions of Ag and ZnO required for this analysis were obtained using the following procedure. Thin layers of the two materials were deposited individually on c-Si substrates while real time spectroscopic ellipsometry (RTSE) data are collected. This procedure allows measurement of accurate bulk layer and surface roughness layer thickness evolution. After each layer has cooled to room temperature, in-situ spectroscopic ellipsometry (SE) data are collected (not in real time). These data along with bulk layer and surface roughness thicknesses are used to calculate the room temperature dielectric functions of each material.

The modeling results in Fig. 2 show the best fit structure of the back reflector. Layers 1 and 2 at the Ag/ZnO interface represent an interface roughness region where layer 2 shows more ZnO character and layer 1 shows more Ag character. The combined thickness of these layers is 335 Å, which is in reasonable agreement with the roughness thickness of the ZnO (300 Å) at the air/ZnO interface. This suggests that the roughness on the starting Ag is transferred to the top of the ZnO through conformal coverage. The additional void density in the ZnO is also reasonable given the very rough surface on which it is deposited. In addition, the thickness of the bulk ZnO is consistent with the nominal (or intended) value of 3000 Å. Although the bulk layer thickness is very close to this value, ZnO also exists within the three roughness layers and the resulting effective thickness from all four contributions is 3402 Å.

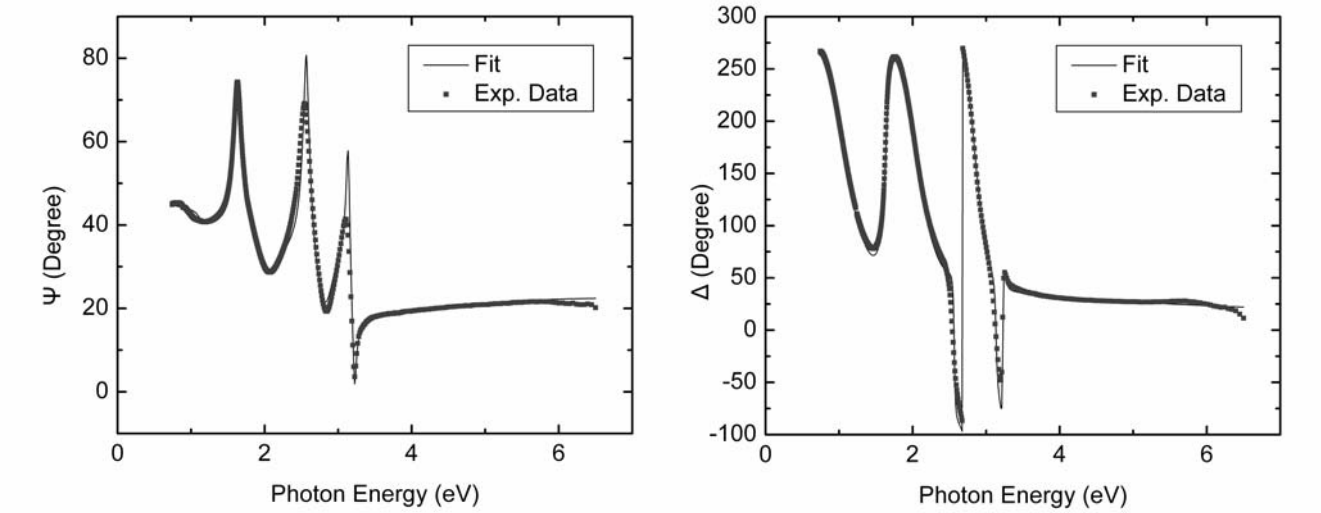

Fig. 1. *Ellipsometric spectra for a Ag/ZnO back-reflector on stainless steel, designed as a light-trapping substrate for a-Si:H-based multijunction solar cells (points). The solid lines represent the results of a best fit model shown in Fig. 2.*

5) Ambient (air)	
4) EMA 68% Zno 32% Void	300Å
3) EMA 95% ZnO 5% Void	2994Å
2) EMA 15% Silver 85% ZnO	204Å
1) EMA 77% Silver 23% ZnO	131Å
0) Silver (optically semi infinite)	3500Å

Fig. 2. *Model used to fit the experimental data of Fig. 1, including semi-infinite Ag at the base, two layers representing the microscopic roughness between Ag and ZnO, a bulk ZnO layer with a density deficit relative to the reference, and a surface roughness layer on the ZnO.*

It is of interest to compare this model to that used for the specular interface layer between smooth Ag and ZnO. The model of Fig. 2 is more complicated due to the fact that two effective medium layers are used at the interface (Ag-rich layer and ZnO-rich layer) rather than one. This was necessary due to the very large thickness of the interface layer. In contrast, however, because the dielectric function of the single layer is determined in the smooth Ag case, the physical characteristics in that case can be understood in terms of the physical processes. Thus, further effort is underway for the textured back-reflector to elicit the physical origins of the losses.

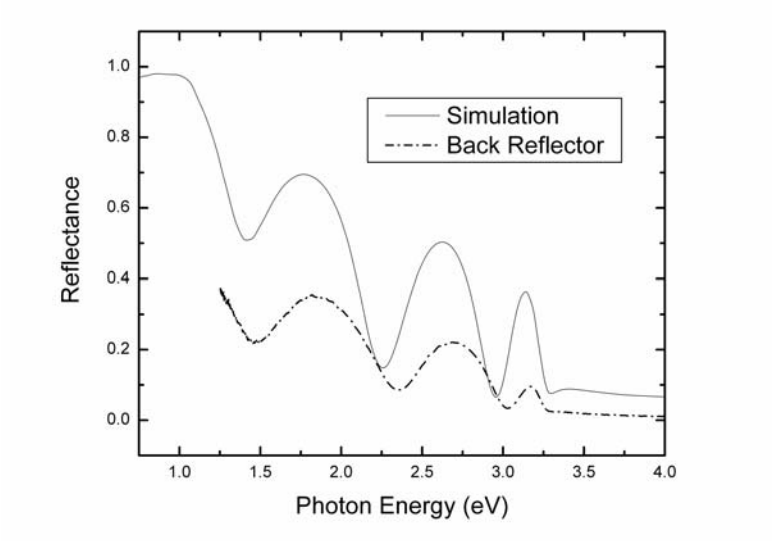

Fig. 3 *Results of simulated and measured specular reflectance of back reflector. The difference shown in Fig. 4 is due to scattered light integrated over all solid angles, i.e., light not collected in a specular measurement.*

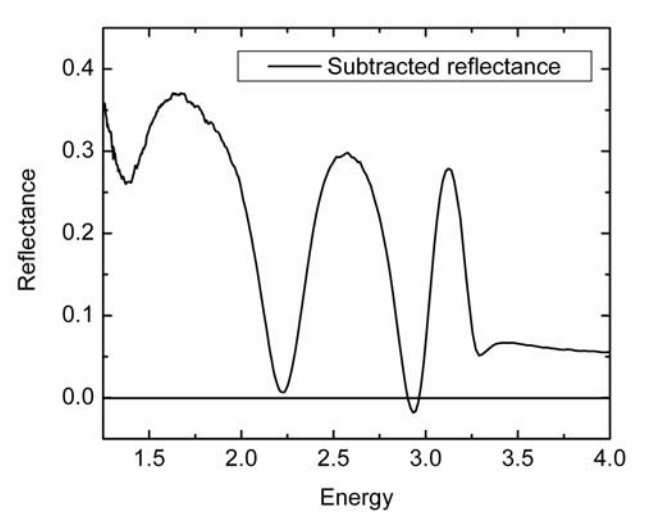

Fig. 4 *Difference between simulated and actual specular reflection which is attributed to scattered light integrated over all solid angles.*

Figure 3 shows the predicted specular reflectance of the back-reflector (solid line) based on the optical model developed in the analysis of Figs. 1 and 2. As demonstrated in the accompanying report on the specular Ag/ZnO interface, the reflectance is nearly unity in the case of an ideal interface. Thus, the significant reduction from unity, modulated by the interface pattern is attributed to interface losses. The results here show the significant role of the interface in generating losses over the range of 1.2 - 1.5 eV. Below 1.2 eV, the predicted refllectance is above 0.9. Further effort is needed to determine the physical mechanism of these losses (e.g., absorption in the Ag component of the interface, or particle or surface plasmon absorption). At this point it is clear that reoptimization is needed even if the desired operating range of the back-reflector is shifted by a small amount (such as the optimum for μc-Si:H bottom cell vs. that for an a-$Si_{1-x}Ge_x$:H bottom cell).

Results and Discussion: Film Growth on Back-reflector

The next steps of depositing the different silicon layers on this back-reflector, lead to a challenging analysis problem whose solution is currently in progress. As an example, Fig. 5 shows the experimental data and fit for the same type of back-reflector, but with a thin ~200 Å a-Si:H n-layer deposited on top. The challenge arises because the thickness of the film is similar to the scale of the roughness layer on the substrate. As a result, the a-Si:H film fills in the roughness layer in the substrate structure while uniformly covering the macroscopic roughness. Although significant improvements of the model are required, the basic concept is demonstrated by the best fit parameters in Fig. 6. In this model, 0.25 of the 0.32 volume fraction of near-surface voids on the ZnO surface are filled with n-layer material (with 0.07 remaining voids). Furthermore a 257 Å layer representing the n-layer surface roughness, resulting from conformal coverage of the ZnO surface appears. Finally, it is noted that the effective thickness of the n-layer

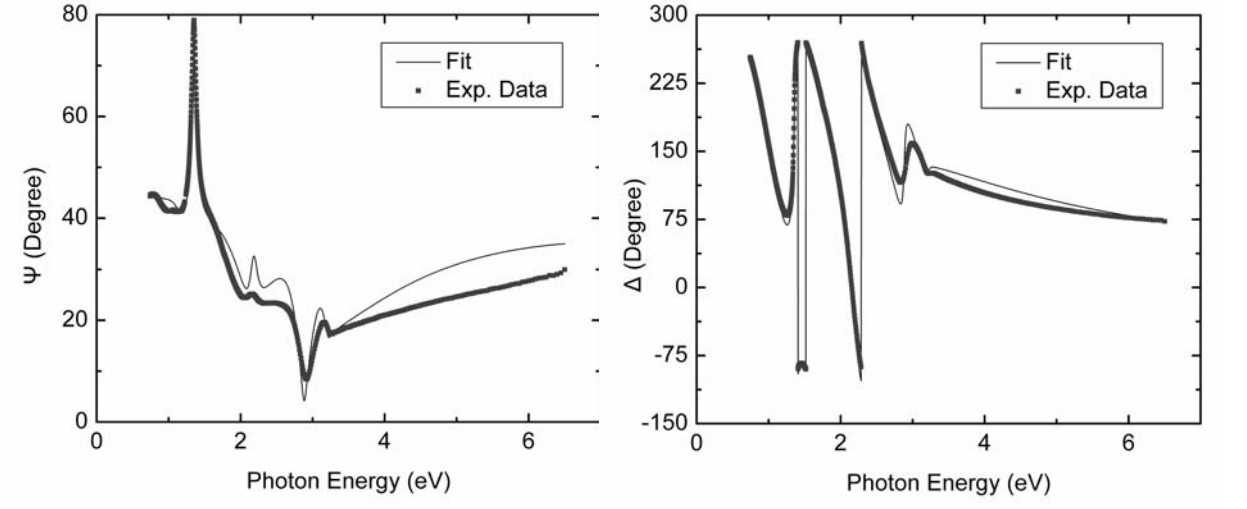

Fig. 5. *Ellipsometric spectra (Ψ,Δ) for a Ag/ZnO/(a-Si:H n-layer) structure, which are the first three layers of an a-Si:H-based multijunction solar cell on a standard back-reflector (points). The solid lines represent the results of the best fit model shown in Fig. 6.*

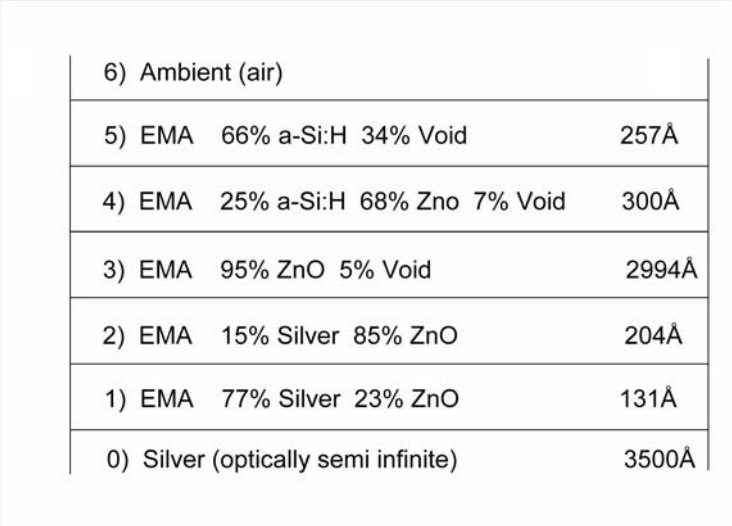

Fig. 6. *Model used to fit the experimental data of Fig. 5 (solid line), including semi-infinite Ag at the base, two layers representing the roughness between Ag and ZnO, a bulk ZnO layer with a density deficit relative to the reference, an interface roughness layer between the ZnO and a-Si:H n-type layer, and finally a surface roughness layer on the n-layer. Note that the n-layer thickness is very close to the thickness of the roughness layer on which it has been deposited, therefore it tracks the underlying roughness layer's morphology.*

including the contributions from the ZnO interface layer and the n-layer surface roughness amount to 245 Å, close to the nominal value of 200 Å.

Future work will involve characterization of single and multijunction a-Si:H-based solar cells on textured back-reflector substrates, including the capability of extracting the i-layer band gaps and crystallite volume fraction for layers intentionally deposited as microcrystalline Si:H.